Optical properties of silicon nanoparticles in the presence of water: A first principles theoretical analysis

D. Prendergast, J.C. Grossman, A.J. Williamson, J.-L. Fattebert, G. Galli

April 15, 2004

Disclaimer

Optical properties of silicon nanoparticles in the presence of water: A first principles theoretical analysis

David Prendergast, Jeffrey C. Grossman, Andrew J. Williamson, Jean-Luc Fattebert and Giulia Galli

Lawrence Livermore National Laboratory, L-415, P.O. Box 808, Livermore, CA 94551.

(Dated: Received June 7, 2004; E-mail: prendergast2@llnl.gov)

We investigate the impact of water, a polar solvent, on the optical absorption of prototypical silicon clusters with oxygen passivation. We approach this complex problem by assessing the contributions of three factors: chemical reactivity; thermal equilibration and dielectric screening. We find that the silanone (Si=O) functional group is not chemically stable in the presence of water and exclude this as a source of significant red shift in absorption in aqueous environments. We perform first principles molecular dynamics simulations of the solvation of an oxygenated silicon cluster with explicit water molecules at 300 K. We find a systematic 0.7 eV red shift in the absorption gap of this cluster, which we attribute to thermal strain of the molecular structure. Surprisingly, we find no observable screening impact of the solvent, in contrast with consistent blue shifts observed for similarly sized organic molecules in polar solvents. The predicted red shift is expected to be significantly smaller for larger Si quantum dots produced experimentally, guaranteeing that their vacuum optical properties are preserved even in aqueous environments.

I. INTRODUCTION

Molecular sensing technology currently relies on fluorescent organic molecules as optical tags. However, these organic dyes have some deficiencies. They absorb light only at specific frequencies, making them inefficient emitters. Their optical emission cannot be tuned readily, and many molecules with unrelated structures and chemistry are required to produce a range of emission wavelengths. Furthermore, prolonged irradiation can lead to chemical or structural decomposition, altering or even destroying desirable optical properties during experiments. These deficiencies may be overcome by using semiconductor quantum dots (QDs) to develop new optical sensing technology.

QDs are pieces of bulk semiconductor in the nanometer-size regime. Their small size bestows them with optical properties that lie somewhere between those of molecules and those of the corresponding bulk materials. Like their bulk counterparts, QDs have robust atomic structures. They absorb light efficiently over a wide range of wavelengths, while emitting light of a characteristic frequency. In addition, due to quantum confinement effects, the optical properties of QDs may be tuned by controlling the size of each nanoparticle. These useful properties make QDs highly competitive with organic dyes for use as optical tags.

QDs made of silicon (Si) are highly desirable, given the abundance of this element and its use in the electronics industry. Also, in contrast with existing QD materials such as cadmium selenide (CdSe), porous silicon (one of the precursors of Si QDs) is both bio-stable and non-toxic. [1] Currently, the use of CdSe QDs as optical tags in biological environments requires coating with many layers of materials, to increase bio-stability, and shield the biological environment from their inherent toxicity. Si QDs do not require any coating and therefore the overall size of Si QDs is typically much smaller than that of coated CdSe QDs. This should permit the use of Si QDs, which possess desirable optical properties and may be applied in aqueous environments, [2] to probe biochemical processes currently inaccessible to CdSe QDs – specifically processes which involve diffusion through intra-cellular membranes.

However, at present, Si QDs of a particular size, synthesized using different approaches, have a large distribution of measured optical properties, e.g. photoluminescence from UV to red. [3] To shed light on the discrepancies between different experiments, first principles calculations have illustrated the important role of surface chemistry [4–10] and structure [11–15] on the optical properties of Si QDs. From this body of work, it is now clear that the optical properties of Si QDs are not determined by size alone.

In this work we analyze the impact of water on the optical absorption properties of Si nanoparticles. In the synthesis process or the application environment, water may be present, in vapor or liquid form, as a solvent or a contaminant. Furthermore, in applications to sensing in biological environments, water would be ubiquitous. Given the known impacts of water – a polar solvent – on the absorption properties of solvated organic molecules, and the absence of equivalent information for inorganic solutes, analysis for Si nanoparticles in water is clearly necessary and important.

II. CONSEQUENCES OF SOLUTE-SOLVENT INTERACTION FOR OPTICAL PROPERTIES

In our study, we consider the solvation of an optically-active species in a polar solvent. The strength of the solute-solvent interaction determines how much the optical properties of the total solvated system deviate from

those of its constituents: the isolated solute and the solvent. If the electronic states involved in optical processes can be clearly associated with the solute (rather than with the solvent) then we may speak of the impact of the solvent on the solute, and that is the focus of this paper. [39] We consider three solute-solvent interactions contributing to changes in the optical properties of the solute: chemical reactivity; thermal equilibration; and dielectric screening.

Dielectric screening refers to the impact on the molecular and electronic structure of the solute due to screening of Coulomb interactions caused by the finite electrical susceptibilities of the solvent and solute. From the electrostatic point of view, this is a self-consistent phenomenon, where the charge density of the solute establishes a polarization of the solvent, which in turn impacts the solute charge density until some equilibrium is reached. Concomitantly, long-range electron correlation leads to attractive dispersion forces between the solute and solvent charge densities. The impact of these screening contributions on optical properties is explained in detail in Sec. III and the impact of screening on the Si clusters studied here is discussed in Sec. VIII. Sections IV and V contain details of our first principles calculations and their application to Si clusters *in vacuo*, respectively.

An investigation of the reactivity of various Si clusters with water is given in Sec. VI. Clearly, if the solute is chemically reactive in the presence of the solvent, the resulting reaction product may have a different molecular structure or composition, and, consequently, a completely different optical signature.

Finally, in Sec. VII we examine the effect of strain induced by thermal fluctuations on optical properties of Si clusters. Thermal equilibration with a reservoir of solvent molecules will activate thermally accessible vibrational modes of the solute. Already, for Si clusters *in vacuo* at zero temperature, there is clear evidence that strain in the molecular structure, e.g. due to surface relaxation, has a large impact on the optical properties of the system. [11, 13, 14]

III. SOLVENT SCREENING AND OPTICAL ABSORPTION

In order to study the impact of water on the optical absorption of Si nanoparticles, it suffices to assess the impact of solute-solvent interactions on the electronic ground state and on the first excited state. The solvation energy [40] may be different for ground and excited states, and this is the origin of so-called solvation shifts (Fig. 1). If the solvation energy of the excited state is larger (smaller) than that of the ground state, we see a red (blue) shift in the absorption energy when compared with the unsolvated system.

One source of this difference in solvation energies is dielectric screening. For a large class of systems, probability distributions of excited state wave functions are more
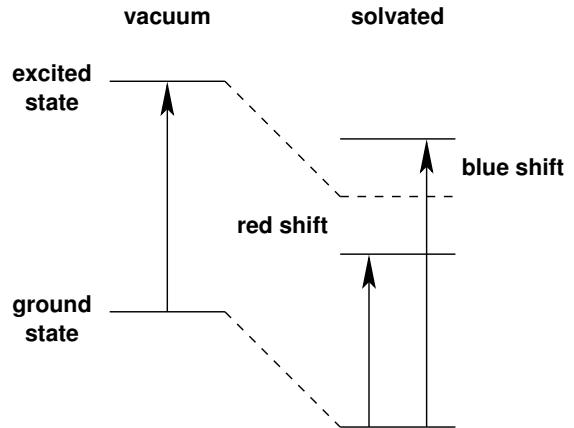

FIG. 1: Schematic energy level diagrams for the electronic states involved in optical absorption for vacuum and solvated systems. Absorption energies required for transitions from ground to excited states are indicated with arrows. The solvation energy causes shifts in the total energy of the ground and excited states. The difference in solvation energies of the ground and excited states leads to a red or blue shift in the absorption energy with respect to the absorption energy *in vacuo*.

diffuse than those of the ground state, and consequently the system has a higher polarizability in the excited state than in the ground state. In general, the more polarizable a system, the larger its solvation energy. Therefore, if the excited state is screened by the solvent, this larger solvation energy will lead to a red shift in absorption. This is often the case for non-polar solvents.

In polar solvents a significant contribution to the screening comes from the alignment of molecular dipoles and occurs on the timescale of molecular motion. Upon absorption of a photon, there is not sufficient time for this orientational polarization to screen the resulting change in the electronic charge density of the solute. Hence, the resulting *non-equilibrium* excited state has a reduced solvation energy with respect to the ground state, leading to an overall blue shift in absorption (Fig. 1).

In practice, both the fast and slow components of the screening response of the solvent are present, leading to a net solvent shift. Water is a highly polar solvent, with an average dipole moment per molecule of ~ 1.9 Debye in the gas phase. The electrical susceptibility of water can be separated into a static component χ_0 and an instantaneous component χ_∞. ($\chi_0 = \epsilon_0 - 1$, where ϵ_0 is the static dielectric constant, and $\chi_\infty = \epsilon_\infty - 1 = n^2 - 1$, where ϵ_∞ is the optical dielectric constant and n is the refractive index). For liquid water at room temperature, $\chi_\infty = 0.78$ and $\chi_0 \sim 77$. Experimental estimates of the Debye relaxation time for water provide an estimate of the time taken for reorganization of the orientational polarization in response to an external electric field. Current theories and experiments agree that there are two Debye relaxation times for water, one fast and one slow. The fast relaxation time has been tentatively associated with single
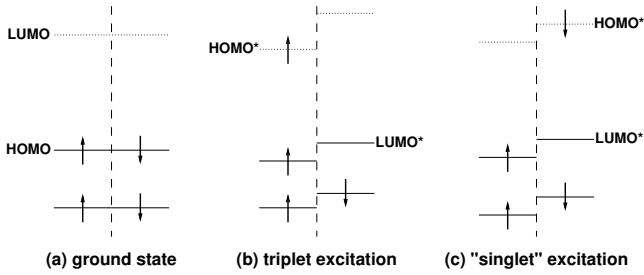
FIG. 2: Schematic energy level diagrams of the electronic states considered in this paper, where single particle orbitals are indicated by horizontal lines, energy increases in the vertical direction, and up and down spin channels are separated with a dashed line. (a) The spin degenerate ground state, indicating the highest occupied molecular orbital (HOMO) and the lowest unoccupied molecular orbital (LUMO). (b) The first excited state with triplet symmetry in a single reference picture, where the highest occupied (lowest unoccupied) molecular orbital of this excited state configuration, labeled HOMO* (LUMO*) can be associated with the LUMO (HOMO) of the ground state. (c) the first excited state used to approximate singlet symmetry, with the HOMO* and LUMO* in the same spin channel.

molecular reorientation and has values from 0.2 – 1.5 ps at ambient conditions. [16, 17] Therefore we can assume that electronic absorption processes (occuring on 0.1 fs time scales) are instantaneous and that the excited states correspond to a non-equilibrium nuclear configuration. In addition, the large difference in magnitudes between χ_∞ and χ_0 increases the energetic cost of the excited state and generally leads to blue shifts in the absorption spectra of optically-active polar organic molecules, e.g. acetone (0.2 eV) [18] and pyridazine (0.5 eV). [19] In this paper, we will see (surprisingly) that these characteristic blue shifts are absent (or at least negligible in the presence of thermal strain) for small inorganic Si clusters (see Sec. VIII).

IV. FIRST PRINCIPLES CALCULATIONS

The optical properties of the various Si clusters examined in this paper are known to be particularly sensitive to their molecular structure. [13] Furthermore, the properties of the solvent and the nature of the solute-solvent interaction can be quite complex, involving charge-transfer, hydrogen-bonding and long-range screening. To capture all of this in our theoretical approach, we need highly accurate estimation of the electronic structure of these systems. For these reasons we adopt first principles computational techniques.

We make use of density functional theory (DFT) under the generalized gradient approximation (GGA). To simulate the impact of finite temperature and explicit solute-solvent molecular interactions, we use first principles molecular dynamics (FPMD), employing the Car-Parrinello method,[20] treating the nuclei in the system

as classical particles acted upon by Coulombic inter-ionic forces and quantum forces derived from the electronic structure.

The majority of electronic structure calculations in this paper were performed using the plane-wave pseudo-potential codes GP [21] and ABINIT. [22] We also used the all electron code GAUSSIAN 98. [23] FPMD simulations were carried out using GP. The DFT/GGA plane-wave pseudo-potential calculations make use of the PBE exchange correlation functional [24] and use a basis of planewaves consistent with periodic boundary conditions on a simulation box of a given size. All calculations are performed for a single point in the Brillouin zone, namely, the Γ-point. In these plane-wave calculations, only valence electrons are included, with atomic cores represented by nonlocal, norm-conserving pseudo-potentials. [25, 26] The Gaussian-basis all electron calculations make use of the Becke functional [27] for exchange and the PW91 correlation functional. [28] These calculations are performed for finite systems using a 6-311G** Gaussian basis set.

A plane-wave kinetic energy cut-off of 70 Ry [41] produces converged results for the electronic structure of the oxygen-containing Si clusters considered here and for water in the condensed phase. For calculations involving Si clusters *in vacuo*, simulation cell dimensions are chosen appropriately to reduce the impact of finite size effects on the results. This is particularly important in calculations on small molecules where the spatial extent of unoccupied electronic states can be much larger than the atomic dimensions of the molecule.

As discussed in Sec. III, to determine the absorption properties of a given system, we require explicit knowledge of the equilibrium electronic ground state and the non-equilibrium excited state. In practice, the absorption spectrum of a physical system is composed of many allowed electronic transitions and associated vibrational transitions. In this paper, we concentrate only on the lowest possible electronic transition in the absence of vibrational excitations. This marks the onset of optical absorption and is equivalent to the band gap of a solid state system. We shall frequently refer to this energy as the absorption gap, E_g. In assessing the impact of water on the optical properties of Si clusters, we assume that a change in the absorption gap is indicative of an overall shift in the absorption spectrum of these systems.

Estimation of the absorption gap using first principles methods can be difficult. Electronic excitations are at heart many-body processes, and so, are difficult to describe using effective single-particle DFT orbitals, especially since most correlation functionals are designed specifically for the electronic ground state. One common DFT estimate of E_g is the difference between the Kohn-Sham eigenvalues of the highest occupied molecular orbital (HOMO) and the lowest unoccupied molecular orbital (LUMO) of the ground state electronic structure [Fig. 2 (a)]. For finite systems *in vacuo*, This HOMO-LUMO gap has been shown, to follow the same trends,

as a function of size, as more accurate estimates of the absorption gap computed using quantum Monte Carlo (QMC) calculations. [29]

However, in determining the impact of dielectric screening on the optical properties of a solvated system, we note that the DFT HOMO-LUMO gap is not an appropriate estimator of the absorption gap. Since the LUMO is never occupied, the HOMO-LUMO gap does not include physical information on the change in solute charge density and corresponding response in solvent polarization upon electronic excitation. For solvated systems, we choose to employ the ΔSCF approach, to determine the absorption gap. Here, we define $E_g = E_{tot}^*(X_0) - E_{tot}(X_0)$, where $E_{tot}^*(X_0)$ is the total excited state energy and $E_{tot}(X_0)$ is the total ground state energy, both evaluated for the ground state molecular structure X_0. By construction, E_{tot}^* includes the impact of electron density variation associated with the solute excited state and any screening impacts from the solvent in response to the solute. The importance of the ΔSCF estimator of E_g for solvated systems is discussed in Sec. IX.

For the systems considered here, the first allowed electronic transition from the ground state is to a state with singlet symmetry. The representation of this singlet state requires more than one reference electron configuration. Since DFT is an effective single particle method we approximate this excitation with the single reference state described in Fig. 2(c). This approximate "singlet" does not have the same symmetry as the true singlet, but it does contain a realistic Coulomb interaction between the states near the Fermi level. Furthermore, a QMC calculation of the absorption gap of the silane molecule (SiH_4) using this single reference approximation has been shown to be accurate to within 0.1 eV. [30]

However, it is well known that numerical convergence of the DFT "singlet" first excited state energy is inherently difficult. A more practicable energy to calculate is that of the first excited electronic state with triplet symmetry [Fig 2 (b)]. This triplet state has a reduced Coulomb energy when compared with the "singlet", due to the exchange repulsion that keeps like-spin electrons apart. For reasons of efficiency and robustness, we choose to compute the ΔSCF estimate of E_g using the triplet excited state. In practice, using either the "singlet" or triplet excited state energy does not qualitatively change our results, and we provide evidence for this in Sec. IX by comparing with some "singlet" state calculations. In the rest of this paper, we shall refer to the "singlet" state without quotation marks.

V. SILICON CLUSTERS IN THE ABSENCE OF WATER

The Si clusters studied in this paper are presented in Fig. 3 and the corresponding estimates of the absorption gaps *in vacuo* are presented in Table I. Despite definite inadequacy in the DFT estimates of the absorption gap,
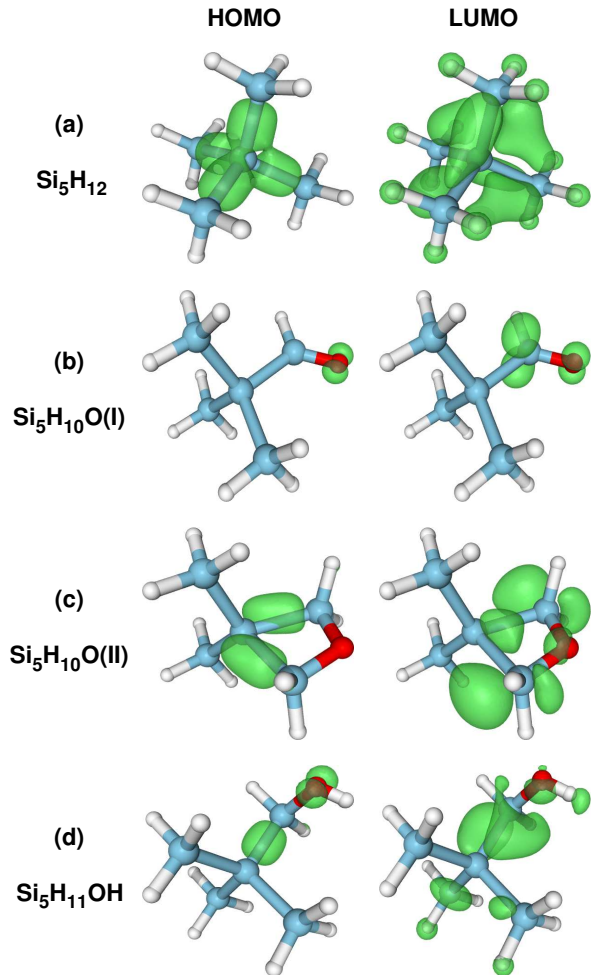

FIG. 3: The structures of various silicon clusters and corresponding probability distributions (green) of the highest occupied molecular orbital (HOMO) and lowest unoccupied molecular orbital (LUMO). All electron density isosurfaces contain 30% of the total charge of the given state. Si atoms are colored blue, O red and H white.

when compared with accurate QMC calculations, there are still consistent trends in comparison of the gaps of Si_5 clusters with different passivants. This has also been demonstrated in previous work over a wide range of Si cluster sizes. [6] Also, the smaller systematic differences between the two sets of DFT gaps are due to the choice of exchange correlation functional and whether the pseudopotential approximation is adopted. We exploit the consistent trends in these calculated gaps, which allow qualitative comparison of the gaps of different systems as long as they are computed using the same level of theory.

Our reference structure is the "pure" hydrogen-saturated Si_5H_{12} [Fig. 3(a)]. We also consider various types of surface passivation containing oxygen. The first, $Si_5H_{10}O(I)$ contains a silanone (Si=O) group [Fig. 3(b)]. The departure from the local tetrahedral symmetry of each Si atom to a planar sp^2 symmetry for the SiHO portion of the molecule produces a localized HOMO and

TABLE I: Absorption gaps (eV) and dipole moments (Debye) for various silicon clusters. Gaps estimated using: HOMO-LUMO DFT/PBE pseudo-potential calculations (PBE-pp); HOMO-LUMO DFT/PW91 Gaussian basis set, all-electron calculations (PW91-ae); and "singlet" ΔSCF QMC calculations (QMC). Dipole moments estimated from PBE-pp charge densities (d_{vac}). Also shown are dipole moments calculated in the presence of a continuum dielectric solvation model for water (d_{solv}) and the angular change in direction (θ) from the unsolvated dipole moment. (The symmetry of Si_5H_{12} guarantees that its dipole moment is zero.)

cluster	E_g			dipole		
	PBE-pp	PW91-ae	QMC	d_{vac}	d_{solv}	θ
Si_5H_{12}	5.8	6.0	6.8	0.0	0.0	0.0°
$Si_5H_{10}O$ (I)	2.9	3.1	3.6	4.5	6.2	8.5°
$Si_5H_{10}O$ (II)	4.5	4.9	5.2	1.6	2.5	3.1°
$Si_5H_{11}OH$	4.7	5.0	5.4	1.2	2.0	4.9°

LUMO on this functional group. The localization effectively creates a defect state within the "band gap" of the molecule reducing the absorption gap by almost 50%. We refer to previous work for a discussion of this effect for Si clusters of various sizes. [6]

We next consider two other forms of oxygen passivation which maintain, to a greater degree, the local tetrahedral symmetry of the Si atoms in the cluster. $Si_5H_{10}O(II)$ contains a bridging oxygen atom between neighboring Si atoms at the surface [Fig. 3(c)]. This causes some strain in the angle between the surface Si atoms bonded to the O and the core Si atom, reducing the tetrahedral angle from the ideal value (109.5°) to 70.4°. However, the preservation of approximate tetrahedral symmetry around each Si atom prevents the same degree of localization of the HOMO and LUMO as we see in $Si_5H_{10}O(I)$. Consequently, the impact on the absorption gap is diminished and, for $Si_5H_{10}O(II)$, E_g is 25% less than that of Si_5H_{12}. $Si_5H_{11}OH$ contains a hydroxyl (OH) passivant, which has a reduced impact on the molecular structure in terms of strain, in comparison with $Si_5H_{10}O(I)$. However, there is still a reduction in the absorption gap due to the electronegativity of the O atom, which attempts to localize the states near the Fermi level around it [Fig. 3(d)].

In a first approximation to the impact of water on the structure of these Si_5 clusters, we use a continuum solvation model [31, 32] to simulate the electrostatic impact of the solvent. We find almost no change in the atomic structure of these molecules in the presence of this solvation model. The most noticeable change is a 1% increase in the bond length of the silanone group in $Si_5H_{10}O(I)$. However, an examination of the impact of this solvation model on the dipole moments of each molecule indicates a consistent tendency to increase the dipole moment (Table I). Given that the atomic structure remains unperturbed in the presence of the solvent polarization, this indicates that the increase in the dipole moment is caused by polarization of the electron charge density.
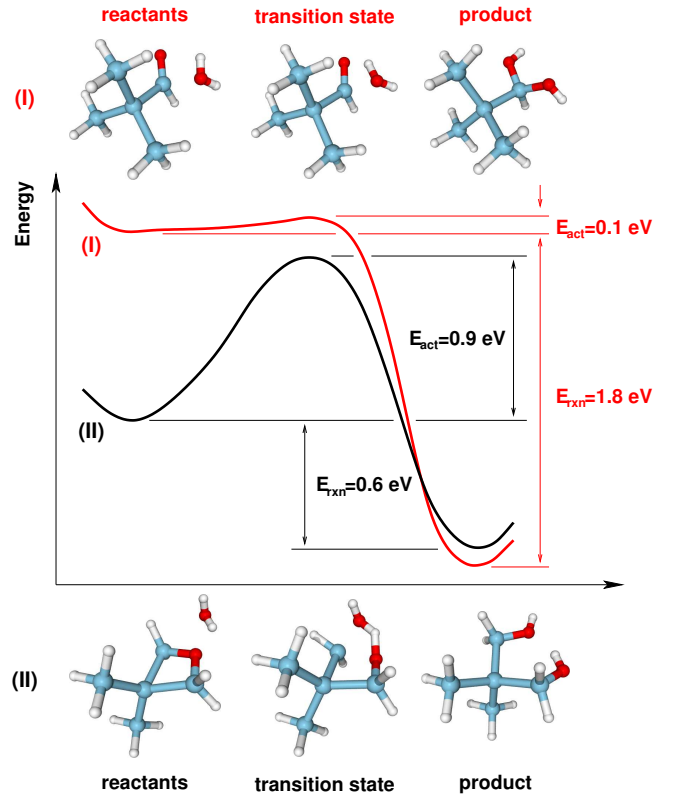

FIG. 4: The reaction paths of $Si_5H_{10}O(I)$ (red) and $Si_5H_{10}O(II)$ (black) with one water molecule, indicating the activation energy E_{act} and the overall energy of reaction E_{rxn}.

TABLE II: Variations in the HOMO-LUMO gap (eV) during the reaction with one water molecule for $Si_5H_{10}O(I)$ and (II). Calculated using PW91-ae.

cluster	reactants	transition state	product
$Si_5H_{10}O$ (I)	3.8	4.0	5.3
$Si_5H_{10}O$ (II)	4.7	4.1	4.7

VI. REACTIVITY OF OXYGENATED SILICON CLUSTERS WITH WATER

The most striking impact of the solvent on a solute would be a chemical reaction producing a more stable chemical species, which we could expect to have quite different optical properties to its precursor. Of the four clusters considered in Section V, $Si_5H_{10}O(I)$ readily reacts with water to produce a dihydroxide according to the reaction:

$$Si_5H_{10}O(I) + H_2O \Rightarrow Si_5H_{10}(OH)_2 \qquad (1)$$
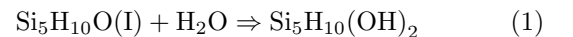
Using GAUSSIAN 98, we determined a 0.1 eV activation energy for this reaction. This involved finding the total energy of the transition state for the reaction, by structural optimization in the direction of the eigenvector of the Hessian matrix with lowest negative eigenvalue.

This reaction profile is compared, in Fig. 4, with the same reaction for the stoichiometrically equivalent bridging structure $Si_5H_{10}O(II)$, which has a larger activation energy of 0.9 eV. This analysis indicates that the survival of silanone groups in water is highly unlikely, given the comparable size of the activation energy with the thermal energy at 300 K (i.e., ~ 0.03 eV). Also, this reaction is exothermic, and the energy released (~ 1.8eV) would fuel the breakdown of other silanone groups by water.

Previous work by Zhou and Head [33] indicates a larger activation energy of 0.3 eV for the silanone group's reaction with water. However, the level of theory (MP2) and smaller system size (one Si atom) in that work may lead to a larger activation energy than the one found here. Furthermore, the 1% increase in the Si=O bondlength in the presence of a polarizable solvent model (Sec. V) indicates that in liquid water this activation energy may be further reduced due to polarization of the $Si_5H_{10}O(I)$ molecule and weakening of the Si=O bond. A recent study of the reactivity of several silica clusters with water by Laurence and Hillier [34], using the B3LYP functional and a comparable basis to ours, reports activation energies of ~ 0.9 eV for the reaction of the Si-O-Si group with water, in good agreement with our result for the reaction of $Si_5H_{10}O(II)$ with a water molecule.

The reaction of $Si_5H_{10}O(I)$ with water leads to a product with a larger absorption gap. The restoration of the local sp^3 symmetry around the Si atom of the Si=O group relaxes the strain on the electronic structure, and the localized states present in the reactant disappear. This increases the DFT HOMO-LUMO gap from 3.8 eV (in the presence of a water molecule) to 5.3 eV, comparable to that of the single hydroxide.

We have also observed this reaction to take place in the course of a FPMD simulation of $Si_5H_{10}O(I)$ in a simulation cell containing 57 water molecules. This reaction occurred while the system temperature was being raised to 300 K, within the first 0.2 ps of the simulation. Therefore, we exclude this cluster from further tests on absorption in the presence of water. Given that the product of this reaction is a hydroxide, which is significantly more stable than the silanone, we regard the hydroxide cluster as a chemically stable species in water.

The absorption gap of $Si_5H_{10}O(II)$ remains essentially the same at 4.7 eV, following the reaction with water. We regard this bridged cluster as chemically stable given its larger activation energy (0.9 eV), and smaller exothermic energy (0.6 eV) in comparison with that of the silanone cluster. Furthermore, as we see in Sec. VII, during a 4.5 ps FPMD simulation we do not observe the hydroxylation of this molecule when solvated in liquid water, despite large fluctuations in the cluster's average kinetic energy which were equivalent to temperatures exceeding 1000 K [Fig. 5(a)].
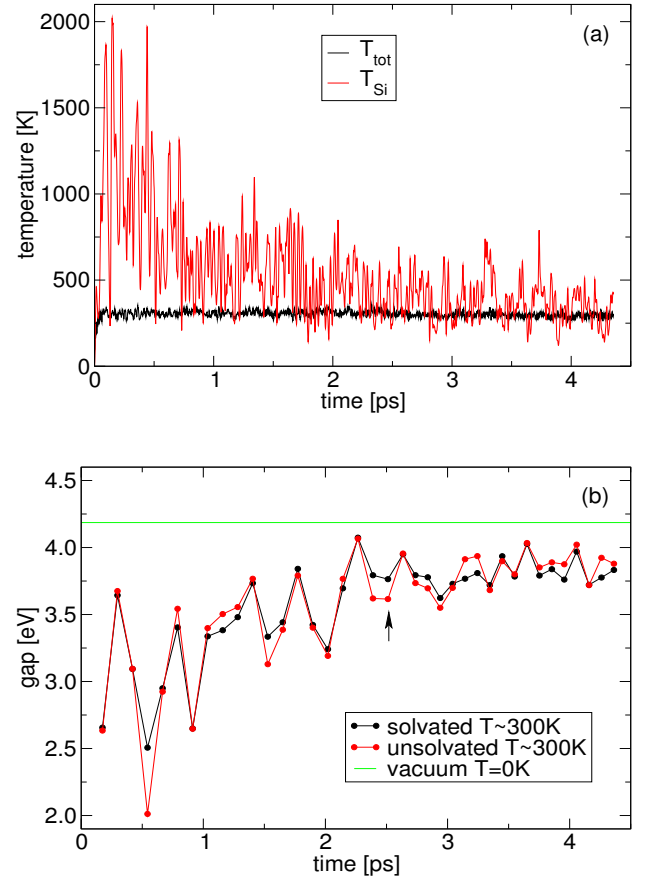

FIG. 5: (a) The system temperature T_{tot} (black) and the instantaneous average kinetic energy (converted to units of temperature) of the Si atoms T_{Si} as a function of time during an FPMD simulation of $Si_5H_{10}O(II)$ in water. (b) The absorption gap of the solvated system (Si cluster and water molecules) computed at the indicated times during the course of the FPMD simulation (black) and the corresponding gap of the same Si cluster structure without the water molecules (red). Also shown is the gap of the Si cluster in its relaxed, zero temperature structure (green). The arrow indicates the particular snapshot used to produce the electronic structure information in Figs. 6 and 7 and Table III.

VII. IMPACT OF FINITE TEMPERATURE ON OPTICAL PROPERTIES OF SILICON CLUSTERS

We simulate the solvation of the molecule $Si_5H_{10}O(II)$ in water using FPMD. The simulation cell dimensions are (12.169 Å × 12.169 Å × 12.169 Å) and the cell contains 57 water molecules in addition to the solute. These cell dimensions were optimized to produce ambient pressure conditions using a classical MD simulation. The final configuration of this classical simulation was used as the starting point of the FPMD run.

The initial 0.17 ps of the FPMD simulation evolve under the influence of a velocity rescaling thermostat after which the temperature of the system reaches 300 K. At this point the thermostat is removed and the simulation

is allowed to evolve with constant total energy. [42]

We notice that the molecular structure of the solute is greatly perturbed during this simulation. This perturbation is caused by the non-equilibrium initial configuration that is used to start the simulation. We assume that the classical forces used to generate this initial configuration have some mismatch with the quantum mechanical forces present in the FPMD simulation. This mismatch greatly increases the average kinetic energy of the solute, as can be seen in Fig. 5(a) (the average kinetic energy of the Si atoms in the solute, T_{Si}, is shown here converted to temperature units for comparison with the system temperature T_{tot}). We see that the solute is effectively equilibrated with the thermal bath of water molecules after 2 ps.

For such a small molecule, it is reasonable to predict that the impact of thermal fluctuations on the structure of $Si_5H_{10}O(II)$ may have a marked impact on its optical properties. From previous work, [11, 13, 14] we know that the impact of strain on Si clusters leads to large red shifts in the absorption gap. This is also observed in our finite temperature simulation. Taking snapshot structural configurations approximately every 0.1 ps from this simulation, we approximate the instantaneous absorption gap as the difference in total energy between the ground state and the triplet first excited state. This is shown in the black curve of Fig. 5(b). It is clear that variations in the absorption gap are highly correlated with the average kinetic energy (or instantaneous "temperature") of the Si atoms, shown in Fig. 5(a). The larger fluctuations in the absorption gap occur at higher temperatures, in the 2 ps equilibration phase of the simulation, where the corresponding structural fluctuations are largest, producing the greatest strain. Once equilibrated, the fluctuations in the gap reach a steady standard deviation of ~ 0.3 eV. The equilibrated system displays a systematic red shift in the absorption gap of 0.7 eV from that of the solute *in vacuo* at 0 K.

VIII. IMPACT OF SCREENING ON OPTICAL ABSORPTION OF SILICON CLUSTERS

The observed 0.7 eV shift is not an effect due to polarization or dispersion from the surrounding solvent molecules. To verify this, we remove the water molecules from each structural configuration used previously and compute the absorption gap of the isolated $Si_5H_{10}O(II)$ molecule. We find that the resulting unsolvated gaps [red curve in Fig. 5(a)] follow the corresponding solvated gaps quite closely. We observe no systematic shift to the red or blue due to the presence of the solvent in the equilibrated phase of the simulation. This is a clear indication that the dominant factor influencing the absorption properties of the solute is the finite temperature of the system.

It is also interesting to note that even in the highly non-equilibrium phase of the simulation of the first 2 ps, structural variations remain the dominant factor in vari-

ations of the absorption gap. In this regime, the solvated and unsolvated gaps are practically the same, while fluctuating over a range of 1.5 eV.

The absence of a systematic solvent shift, due to screening, for the Si cluster in water is at variance with the solvent shifts of polar organic solutes in polar solvents, where an experimentally observed blue shift in the absorption gap is expected from screening arguments. Recent calculations by Bernasconi *et al.*[18] have shown that a solvent blue shift for acetone in water is resolvable from a relatively short FPMD simulation. This contrast with our results is interesting and may point to fundamental differences between organic and inorganic solutes in water.

IX. ELECTRONIC STRUCTURE

We analyze the electronic structure of the solvated system described in Sec. VII in order to assess the validity of our approach to the calculation of absorption gaps, and to deduce why dielectric screening does not have a large impact on the optical properties. Figure 6 illustrates the charge density associated with several Kohn-Sham eigenstates near the Fermi level, for an isolated Si cluster (unsolvated), for the Si cluster surrounded by water (solvated) and for a configuration taken from a FPMD liquid water simulation at 300 K (water).

We examine first the states illustrated in Figure 6(e)-(h). We notice that the HOMO of the solvated system [Figure 6(e)] is localized on the Si cluster solute. This localization of the HOMO is typical for each of the configurations examined in Fig. 5. This is in contrast with, e.g., the acetone-water system examined by Bernasconi *et al.* [18] In that work, the HOMO varied in its localization during the course of a FPMD simulation, at times reminiscent of the HOMO of the isolated acetone system, and at others more like the HOMO of water in the condensed phase.

The LUMO of the solvated system [Figure 6(f)] is entirely delocalized over the simulation cell. However, when we alter the occupancy of the Kohn-Sham eigenstates (as described in Sec. IV) to produce the singlet or triplet first excited states, we notice that the HOMO* – the analogue of the LUMO in the occupied excited state – is localized on the solute. In comparison with the localized states of the unsolvated Si cluster shown in Figure 6(a)-(d), only the LUMO of the solvated system differs significantly.

Our initial motivation for considering occupied excited state configurations was to capture the screening response of the solvent to variations in the solute charge density from its electronic ground state. We find that the physically different charge distributions associated with the LUMO and HOMO* of this solvated system are not significant for the various estimates of the absorption gap. We see from Table III that the HOMO-LUMO estimate is essentially the same as the ΔSCF singlet estimate.

Our use of the triplet excited state, for reasons of ef-

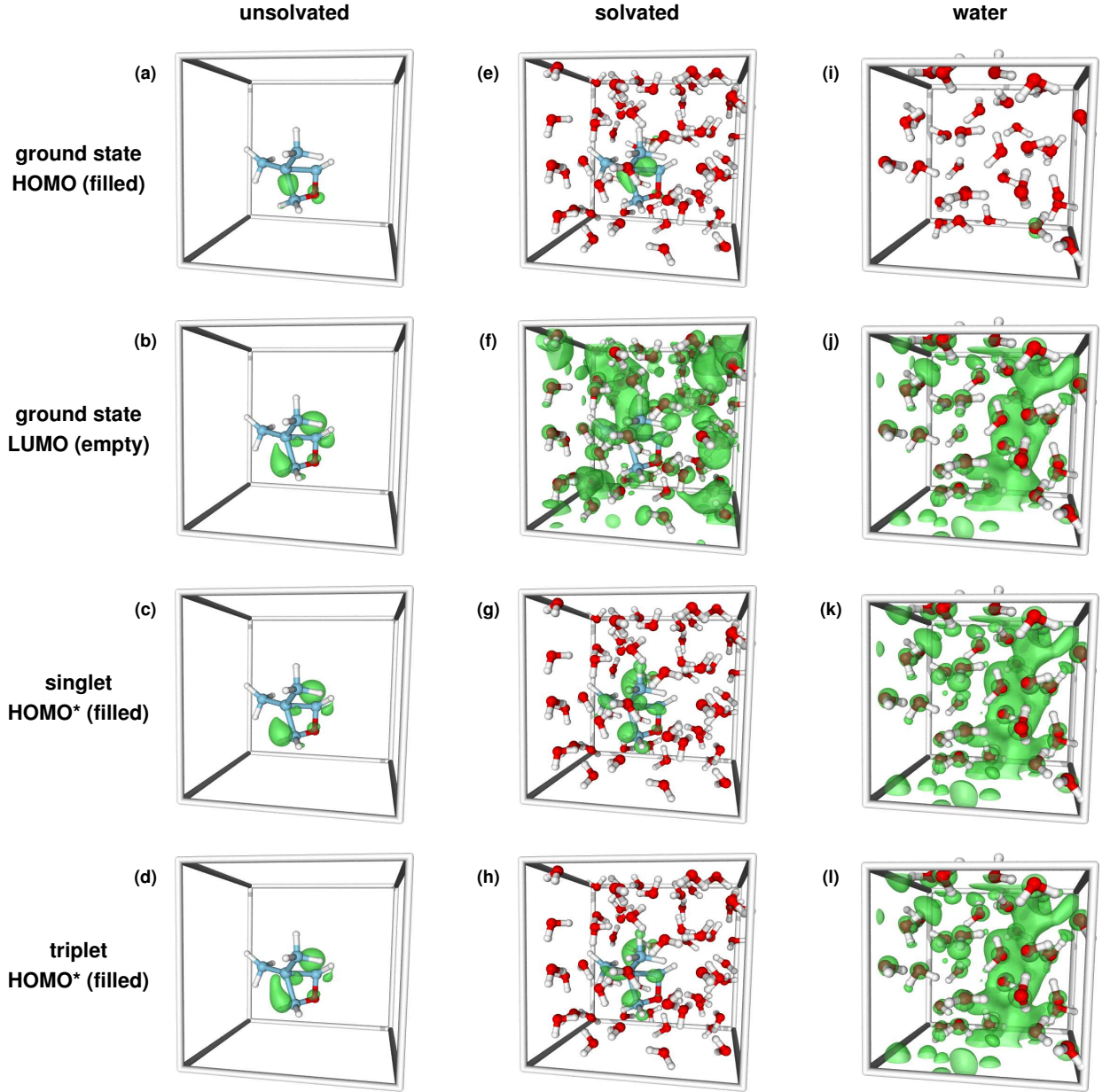| unsolvated	solvated	water

FIG. 6: The electronic structure of various Kohn-Sham eigenstates near the Fermi level for a specific configuration chosen at the 2.5 ps point from the FPMD simulation of $Si_5H_{10}O(II)$ in water outlined in Fig. 5. The unsolvated systems (a)-(d) contain equivalent solute structures to the solvated systems (e)-(h), but have all water molecules removed. Also displayed (i)-(l) are states near the Fermi level for a configuration taken from an FPMD simulation of water at 300 K. All charge density isosurfaces (green) contain 30% of the total charge of the given state. Atom colors are as indicated in Fig. 3.

ficiency (Sec. IV), is justified by the close physical resemblance of the charge densities of the HOMO* in each case. The splitting between the singlet and triplet ΔSCF absorption gaps can be associated with exchange effects local to the Si cluster, since the relevant gap states are localized on the cluster and the presence of water or the perturbation of the molecular structure has little effect on this splitting, which remains ~ 0.2 eV in all cases.

However, the difference between the LUMO and HOMO* has important consequences for other physical quantities, such as the oscillator strength (f) for this transition. We find that for the HOMO-LUMO transition, $f = 0.05$, while for the transition from LUMO* to HOMO*, $f = 0.60$ (refer to Fig. 2(b) for definitions of these states). Using the LUMO* is justified given its almost complete (99.8%) overlap with the HOMO of the ground state. This order of magnitude difference in f will have important consequences for calculated optical absorption.

The delocalization of the LUMO of the solvated sys-

TABLE III: Various DFT estimates of the absorption gap for the $Si_5H_{10}O(II)$ molecule: in its vacuum, zero temperature structure; at 300 K *in vacuo*; and at 300 K in water. The finite temperature estimates of the gap use the molecular structure of the snapshot considered in Fig. 6. Also shown is the splitting between the singlet and triplet ΔSCF estimates of the gap. All energies given in eV.

Phase	vacuum	vacuum	solvated
Temp (K)	0	300	300
HOMO-LUMO	4.5	3.7	3.9
ΔSCF singlet	4.4	3.8	3.9
ΔSCF triplet	4.2	3.6	3.8
singlet-triplet	0.19	0.18	0.17

tem [Fig. 5(f)] is reminiscent of the delocalized LUMO observed in previous DFT calculations of the electronic structure of liquid water. [35, 36] An example of this LUMO of water is provided in Fig. 6(j). To interpret the origin of various states near the Fermi level of the solvated system, we compare its density of states (DOS), in Fig. 7, with that of the unsolvated system and that of pure liquid water. The energy scale in this figure is shifted in such a way that the HOMO of the solvated system is at zero. Given that the HOMO and LUMO of the solvated system are qualitatively similar to the HOMO of the isolated solute and the LUMO of pure water, respectively, we choose to align these pairs of states for the sake of comparison. It is worth noting that this seemingly arbitrary alignment is consistent for other effective single-particle states. For example, the lowest valence *s* states of the oxygen atoms in each system are correctly aligned at around ~ -20 eV on this energy scale (this part of the DOS has been omitted for clarity in Fig. 7). We also note that the isolated LUMO of liquid water, shown at ~ 2.5 eV in Fig. 7(c), is the subject of some controversy and may not reflect a physically observable transition. [18, 37]

The DOS of the unsolvated Si cluster indicates another state quite close in energy to the LUMO of the solvated system, and, in fact, the LUMO+1 Kohn-Sham eigenstate of the solvated system resembles this unsolvated, localized, empty state. This is also true of the HOMO* of the singlet and triplet configurations. Therefore we conclude that occupying the first excited state leads to a reordering of states near the Fermi level, such that the delocalized LUMO is replaced by a localized HOMO*. The preference for a localized HOMO* is due to the binding energy associated with the underlying charge distribution, which contains a "hole" (unoccupied LUMO*) localized on the Si cluster. To further illustrate this point, we see that for the states near the Fermi level in liquid water [Fig. 6(i)-(l)] there is no significant difference between the charge densities of the LUMO and HOMO*. There is no localized state nearby in energy in the conduction band with which to swap, and also there is no localized "hole" to favor such a reordering of energy lev-
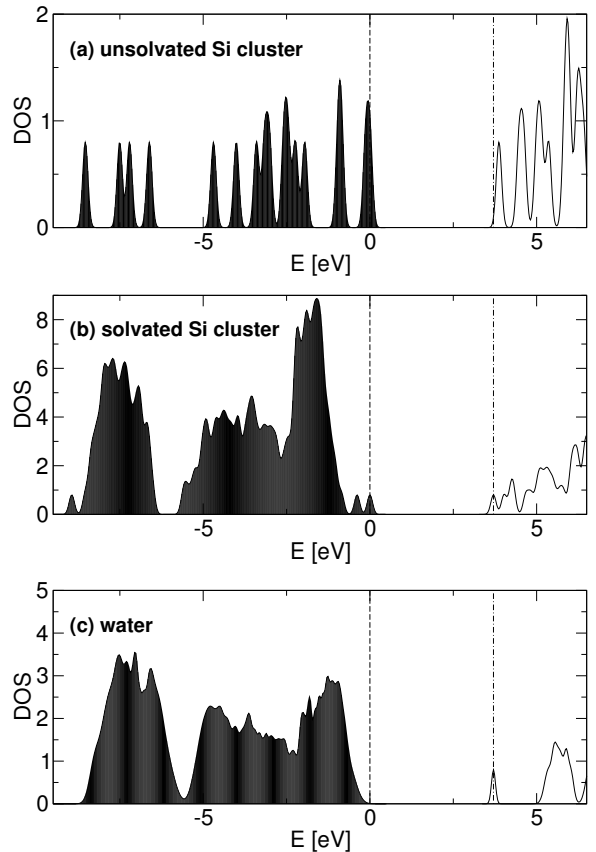

FIG. 7: The density of states (DOS) of (a) the unsolvated Si cluster of Fig. 6(a); (b) the solvated Si cluster of Fig. 6(e); and (c) that of liquid water. The DOS of water was calculated by thermal averaging over 20 ps of a FPMD simulation of 32 water molecules at ambient pressure and 300 K. The average broadening of states for this simulation was 0.08 eV which was then used to broaden the discrete spectra of (a) and (b). The energy scale in (b) is shifted to place the HOMO at zero (vertical dashed line). The shift in energy applied to (a) places the HOMO at zero also, while the shift applied to (c) aligns the LUMO with the LUMO of (b) (vetical dashed-dotted line). The oxygen *s*-states have been omitted, but lie at ~ -20 eV.

els.

X. CONSEQUENCES FOR EXPERIMENT AND THEORY

There are several conclusions that experimentalists may draw from our computations. With regard to reactivity, we see that for absorption processes, the existence of the silanone group is very unlikely, given its low activation energy for reaction with water. Note that the existence of a photostable silanone in the presence of water, proposed by Zhou and Head, [33] is only relevant for emission processes. Also, other work [9] indicates that the significant red shift induced by this functional group may be reproduced by complete passivation with other

types of oxygen containing groups, such as hydroxyls and bridging oxygens.

We expect that the large red shift caused by thermal strain in our finite temperature simulations (Fig. 5) may be more pronounced for this small prototypical cluster than it would be for a larger Si QD. For larger Si QDs, with more rigid surface reconstructions, we expect that finite temperature effects will play a smaller role in their impact on the absorption gap. This is further reinforced by the small temperature dependence of the lowest direct gap of bulk Si, which shifts to the red by only ~ 0.05 eV upon increasing the temperature from 0 K to 300 K. [38]

The lack of any screening impact on the absorption of such a small Si cluster, with a relatively large dipole moment indicates that for larger Si QDs, this effect may also be negligible. The likelihood of complete passivation of the surface of a large Si QD with oxygen will significantly reduce the total dipole moment of such particles. Furthermore, the preference for oxygen containing passivants which effectively preserve the local tetrahedral symmetry around each Si atom guarantees that the electronic states near the Fermi level are delocalized over the entire QD. Therefore, screening impacts are reduced, given that they are more likely to be limited to the surface region of the QD, not extending far into the core. However, in larger Si QDs a smaller red shift due to thermal strain may permit the observation of small solvent shifts due to screening. This issue requires further investigation.

For theorists, it seems that simulating solvated Si QDs may not require large FPMD simulations which include water. Given that the screening impact is so small, there may be no advantage to including many solvation shells of water molecules in a simulation. On the other hand, analysis of ground state structures and active vibrational modes at a given finite temperature may provide more useful information than large finite temperature simulations and thermodynamic averaging.

XI. CONCLUSIONS

This is the first theoretical analysis of the impact of aqueous solvation on the optical properties of Si nanoparticles. While there have been many studies on the impact of polar solvents on the absorption properties of organic molecules, so far no investigation has been reported for inorganic solutes such as QDs. In our analysis we considered three factors: chemical reactivity; thermal equilibration; and dielectric screening. Regarding chemical reactivity, we find that the silanone functional group is extremely reactive in the presence of water and is unlikely to exist in aqueous solvation. We find that the bridging oxygen and hydroxide surface passivants are much more stable and therefore more probable sources of red shifts in the experimentally observed absorption spectra. At 300 K, we find that thermal fluctuations induce strain in the small silicon cluster examined here, and we estimate that this strain leads to a systematic red shift of ~ 0.7 eV. Upon removing the screening impact of the surrounding water, we determine no noticeable impact of solvent polarization or dispersion on the optical absorption gap of this silicon cluster. Given the thermal stability of larger QDs, we conclude that chemically stable Si QDs will have robust optical properties in the presence of water, further justifying their use as stable and efficient optical tags in biological sensing applications.

[1] Mayne, A. H.; Bayliss, S. C.; Barr, P.; Tobin, M.; Buckberry, L. D. *Phys. Sat. Sol. (a)* **2000**, *182*, 505-513.

[2] Harwell, D. E.; Croney, J. C.; Qin, W.; Thornton, J. T.; Day, J. H.; Hajime, E. K.; Jameson, D. M. *Chem. Lett.* **2003**, *32*, 1194-1195.

[3] Wilcoxon, J. P.; Samara, G. A.; Provencio, P. N. *Phys. Rev. B* **1999**, *60*, 2704-2714.

[4] Filonov, A. B.; Ossicini, S.; Bassani, F.; d'Avitaya, F. A. *Phys. Rev. B* **2002**, *65*, 195317.

[5] Vasiliev, I.; Chelikowsky, J. R.; Martin, R. M. *Phys. Rev. B* **2002**, *65*, 123102.

[6] Puzder, A.; Williamson, A. J.; Grossman, J. C.; Galli, G. *Phys. Rev. Lett.* **2002**, *88*, 097401.

[7] Puzder, A.; Williamson, A. J.; Grossman, J. C.; Galli, G. *J. Chem. Phys.* **2002**, *117*, 6721-6729.

[8] Puzder, A.; Williamson, A. J.; Grossman, J. C.; Galli, G. *J. Am. Chem. Soc.* **2003**, *125*, 2786-2791.

[9] Zhou, Z. Y.; Brus, L.; Friesner, R. *Nano. Lett.* **2003**, *3*, 163-167.

[10] Zhou, Z. Y.; Friesner, R. A.; Brus, L. *J. Am. Chem. Soc.* **2003**, *125*, 15599-15607.

[11] Weissker, H. C.; Furthmuller, J.; Bechstedt, F. *Phys. Rev. B* **2003**, *67*, 245304.

[12] Vasiliev, I.; Martin, R. M. *Phys. Stat. Sol. B* **2002**, *233*, 5-9.

[13] Puzder, A.; Williamson, A. J.; Reboredo, F. A.; Galli, G. *Phys. Rev. Lett.* **2003**, *91*, 157405.

[14] Draeger, E. W.; Grossman, J. C.; Williamson, A. J.; Galli, G. *Phys. Rev. Lett.* **2003**, *90*, 167402.

[15] Draeger, E. W.; Grossman, J. C.; Williamson, A. J.; Galli, G. *J. Chem. Phys.* **2004**, in press.

[16] Gaiduk, V. I. *Opt. Spectrosc.* **2003**, *94*, 199-208.

[17] Buchner, R.; Barthel, J.; Stauber, J. *Chem. Phys. Lett.* **1999**, *306*, 57-63.

[18] Bernasconi, L.; Sprik, M.; Hutter, J. *J. Chem. Phys.* **2003**, *119*, 12417-12431.

[19] Baba, H.; Goodman, L.; Valenti, P. C. *J. Am. Chem. Soc.* **1966,** *88,* 5410-5415.

[20] Car, R.; Parrinello, M. *Phys. Rev. Lett.* **1985,** *55,* 2471-2474.

[21] Gygi, F. "GP, a general *ab initio* molecular dynamics program", Lawrence Livermore National Laboratory, Livermore, California, 2003.

[22] Gonze, X. *et al. Computational Materials Science* **2002,** *25,* 478-492 The ABINIT code is a common project of the Université Catholique de Louvain, Corning Incorporated, and other contributors (URL http://www.abinit.org).

[23] Frisch, M. J. *et al.* "GAUSSIAN 98, Revision A.7", Gaussian, Inc., Pittsburgh PA, 1998.

[24] Perdew, J. P.; Burke, K.; Ernzerhof, M. *Phys. Rev. Lett.* **196,** *77,* 3865-3868.

[25] Hamann, D. R. *Phys. Rev. B* **1989,** *40,* 2980-2987.

[26] Troullier, N.; Martins, J. L. *Phys. Rev. B* **1991,** *43,* 1993-2006.

[27] Becke, A. D. *Phys. Rev. A* **1988,** *38,* 3098.

[28] Wang, Y.; Perdew, J. P. *Phys. Rev. B* **1991,** *43,* 8911-8916.

[29] Williamson, A. J.; Grossman, J. C.; Hood, R. Q.; Puzder, A.; Galli, G. *Phys. Rev. Lett.* **2002,** *89,* 196803.

[30] Grossman, J. C.; Rohlfing, M.; Mitas, L.; Louie, S. G.; Cohen, M. L. *Phys. Rev. Lett.* **2001,** *86,* 472-475.

[31] Fattebert, J.-L.; Gygi, F. *J. Comput. Chem.* **2002,** *23,* 662.

[32] Fattebert, J.-L.; Gygi, F. *Int. J. Quant. Chem.* **2003,** *93,* 139.

[33] Zhou, F.; Head, J. D. *J. Phys. Chem. B* **2000,** *104,* 9981-9986.

[34] Laurence, P. R.; Hillier, I. H. *Comp. Mater. Sci.* **2003,** *28,* 63-75.

[35] Laasonen, K.; Sprik, M.; Parrinello, M. *J. Chem. Phys.* **1993,** *99,* 9080-9089.

[36] Boero, M.; Terakura, K.; Ikeshoji, T.; Liew, C. C.; Parrinello, M. *J. Chem. Phys.* **2001,** *115,* 2219-2227.

[37] Blumberger, J.; Bernasconi, L.; Tavernelli, I.; Vuilleumier, R.; Sprik, M. *J. Am. Chem. Soc.* **2004,** *126,* 3928-3938.

[38] Allen, P. B.; Cardona, M. *Phys. Rev. B* **1983,** *27,* 4760-4769.

[39] This picture is analogous to optically-active point defects in solids, where defect states are introduced within the optical band gap of the solid, such that the optical properties of the combined system can be attributed to the defect rather than to the solid.

[40] The solvation energy is defined as $[E(\text{solute}) + E(\text{solvent})] - E(\text{solute} + \text{solvent})$, where $E(\text{solute})$ is the total energy of the isolated solute; $E(\text{solvent})$ is the total energy of the pure solvent; and $E(\text{solute} + \text{solvent})$ is the total energy of the solvated system.

[41] In practice, we use a plane-wave cut-off of 69 Ry, which leads to more efficient grid dimensions for fast Fourier transforms.

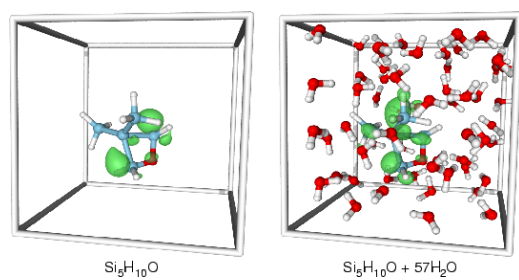[42] For the final 1.5 ps of the simulation the time step is increased to 3 a.u, while the fictitious electron mass was kept fixed at 276 a.u.

FIG. 8: Table of Contents Figure.